

## Relating density and elastic velocities in clastics: an observation

Colin C. Potter

### ABSTRACT

This preliminary work examines the relationship between density ( $\rho$ ), P-wave ( $V_p$ ) and S-wave ( $V_s$ ) velocity logs in different clastics, using Gardner's empirical relationship and investigates how well measured densities compare to it. Deviations from Gardner's equation were large and systematic and can be possibly related to other factors, such as lithology, porosity, and pore fluids. The log data is from four wells in the Blackfoot field in south central Alberta. The Upper Mannville and Glauconitic members of the Lower Cretaceous are the targets of this observation. Preliminary cross plots of different measured and calculated logs within these zones give estimates of possible empirical relationships.

### INTRODUCTION

This paper investigates the relationship between density and velocities pertaining to equations (1) and (2) and how porosity and lithology affect these relationships. The log data studied in this report are from the 08-08, 100/09-08, 04-16, and 12-16 wells located in the Blackfoot field of Twp. 23, Rng. 23 W.4 in Alberta. The Glauconitic member of the Mannville Group in southern Alberta is the zone of interest. This consists of very fine to medium quartz sandstone in an incised valley system. This incised valley is subdivided into three phases of valley incisions. The upper and lower channels consist of porous quartz sandstones, while the middle channel consists of relatively denser lithic sandstone. The Upper Mannville member consists of a combination of sandstones, siltstones, and shales. The Glauconitic and Upper Mannville members are the targets of this investigation.

Relating density and velocity has always been a useful correlation in the oil and gas sector. The product of density and velocity is needed for elastic impedance, which in turn is required for seismic reflection work. When density is not available it is often estimated from P-wave velocity using Gardner's relationship (Gardner et al., 1974). This relationship that was deduced from a series of controlled field and laboratory measurements of saturated sedimentary rocks from various locations and depths is:

$$\rho = aV^b \quad (1)$$

where  $\rho$  is in  $\text{g/cm}^3$ ,  $a$  is 0.31 when  $V$  is in m/s and is 0.23 when  $V$  is in ft/s and  $b$  is 0.25. As shown in Figure 1, this relationship is an average of the trends of major sedimentary rocks, while coals and evaporites do not conform to this trend.

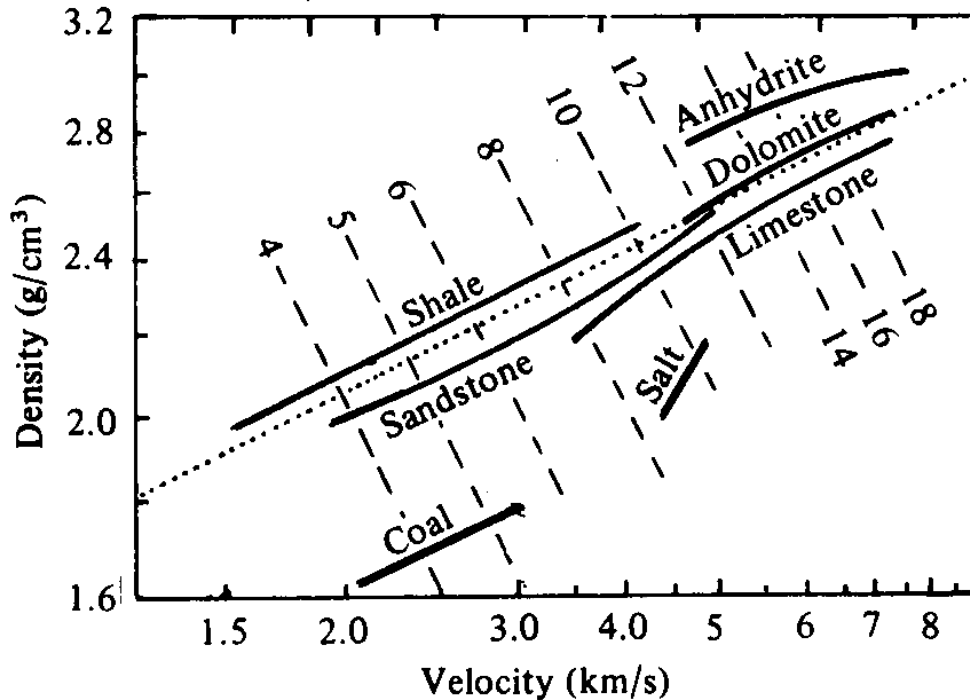


Figure 1. Density versus P-wave velocity (log-log scale). Gardner's empirical relationship where the dotted line pertains to equation (1) (from Sheriff and Geldart, 1995)

Potter and Stewart (1990) found an empirical relationship between S-wave velocity and density replicating Gardner's relationship:

$$\rho = 0.37 V_s^{0.22} \quad (2)$$

where  $\rho$  is in  $\text{g/cm}^3$  and  $V_s$  is in  $\text{ft/s}$ .

Poisson's ratio ( $\sigma$ ) is an elastic constant that can improve lithology, porosity, and pore fluid predictions (e.g. Pickett, 1963; Rafavich, 1984; Miller and Stewart, 1990).  $\sigma$  is described as the ratio of fractional transverse contraction to the fractional longitudinal extension when a rod is stretched (Sheriff, 1991).  $\sigma$  is generally low in stiff materials and higher in less rigid materials.

## METHODS

The wells investigated in this paper were selected because they have dipole sonic logs. These logs have intervals that range from above the Upper Manville member to the Shunda-Mississippian member. All logs were obtained from the QCData well log database, since data received from PanCanadian Petroleum did not have porosity logs. The dipole sonic logs from PanCanadian have been processed and true vertical depth (TVD) corrected, while the logs from QCdata have not been corrected. This is evident when comparing S-wave sonics from the two different sources. The slowness values of the Shear Delta-T logs from QCData are lower than the S-wave Sonic logs from PanCanadian. These values range from 5% lower overall up to 15% lower for some spikes. The P-wave sonics and the bulk density logs from both sources are

comparable. The lower S-wave sonic values affect the calculated elastic constants, since P-wave, and S-wave velocities, and density values are required to calculate the elastic parameters.

The logs from QCData were resampled to 0.3048m/sample and edited for spikes caused by borehole washout. Tops were picked on all logs corresponding to those used by PanCanadian. The MATLAB scientific programming environment was used to edit and calculate logs, pick tops and obtain the cross-plots, diagrams, and estimated coefficients. Intervals pertaining to different formations for each well were indexed, so these intervals for the different wells could be cross-plotted against each other. The MATLAB function 'polyfit' was used to obtain the coefficients of the polynomial that best fit the data in a least squares sense. Then, the function 'polyval' was used to evaluate the polynomial at all values of the x-axes so the best-fit line could be plotted.

When relating density with velocities, equation (1) was used in a log-log sense. A linear equation is obtained

$$\log(\rho)=b*\log(V)+\log(a). \quad (3)$$

The cross-plots are linear relationships between different logs and elastic parameters for the Upper Mannville and the Glauconitic members of the Mannville Group, where observations of the results were noted.

## RESULTS

The first set of cross-plots represented are log density versus log velocities relating to equation (3). The symbols and best-fit lines for the different wells on all plots are as follows:

- 08-08 circle o solid line - ;
- 09-08 star \* dashed line -- ;
- 04-16 square □ dashed line -- ;
- 12-16 diamond ◇ dash dot line -. ;

For all equations derived from data in this paper, velocities are in m/s and density is bulk density in g/cm<sup>3</sup>, unless otherwise specified.

Figure 2 shows the logarithm density versus the logarithm of P-wave velocity for the 08-08, 09-08, 04-16, and 12-16 wells for the Mannville (MANN) and shows the best-fit lines for each wells. The equations derived for this data are as follows:

$$08-08 \quad \rho=0.46V_p^{0.05} \quad (4)$$

$$09-08 \quad \rho=0.35V_p^{0.13} \quad (5)$$

$$04-16 \quad \rho=0.24V_p^{0.33} \quad (6)$$

$$12-16 \quad \rho=0.31V_p^{0.19} \quad (7)$$

$$\text{all wells} \quad \rho=0.34V_p^{0.15} \quad (8)$$

The coefficients in equations (4) to (8) differ from those in of Gardner's equation. Although there is a difference in the coefficients, the values for 'all wells' do not deviate greatly from those of Gardner's. The coefficient of 0.34 for 'all wells' is close to that of Gardner's value of 0.31, but the exponent coefficient of 0.15 differs substantially. This plot indicates that Gardner's equation agrees fairly well with the measured values for 'all wells'. The data points for all four wells are scattered, but still have a definite trend. The data for the 12-16 well represents Gardner's equation best.

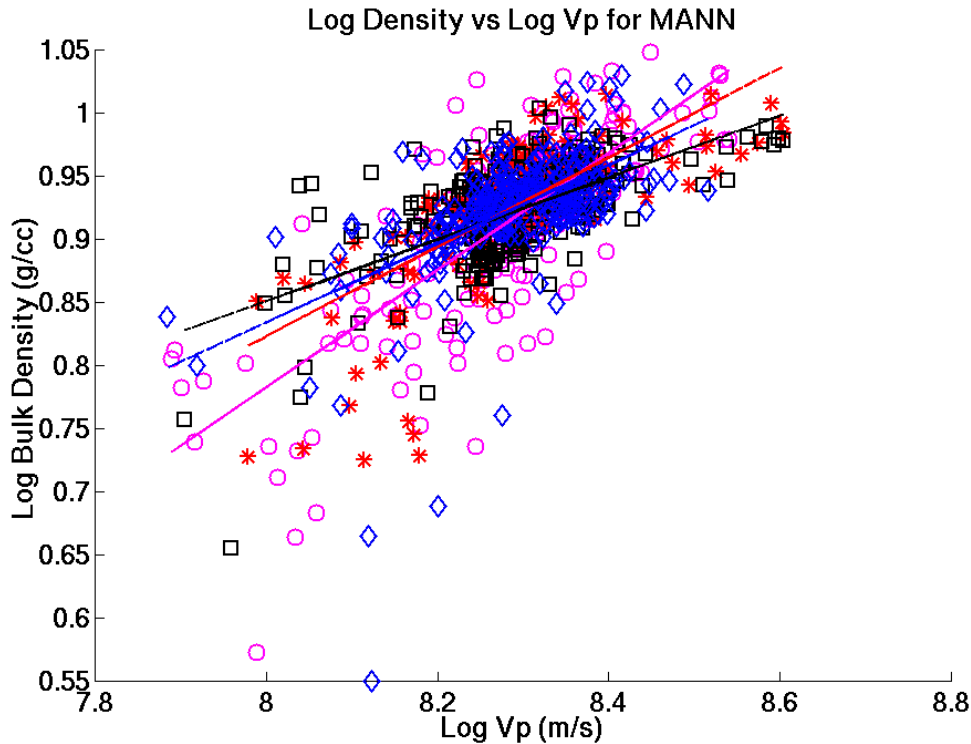


Figure 2. Log density versus log  $V_p$  for the 08-08 (O), 09-08 (\*), 04-16 ( $\square$ ), and 12-16 ( $\diamond$ ) wells for the Mannville.

Figure 3 shows the logarithm density versus the logarithm of S-wave velocity for the 08-08, 09-08, 04-16, and 12-16 wells for the Mannville (MANN) and shows the best-fit lines for each wells. The equations derived for this data are as follows:

$$08-08 \quad \rho=0.25V_p^{0.37} \quad (9)$$

$$09-08 \quad \rho=0.19V_p^{0.62} \quad (10)$$

$$04-16 \quad \rho=0.20V_p^{0.56} \quad (11)$$

$$12-16 \quad \rho=0.32V_p^{0.22} \quad (12)$$

$$\text{all wells} \quad \rho=0.24V_p^{0.41} \quad (13)$$

The data for this plot are widely scattered, but still have apparent trends. This scattering is probably due to the slightly less reliable values of the Vs logs. When comparing the equations (9) to (13) with equation (2), the data for the 12-16 well fits best after the Vs data was converted to ft/s.

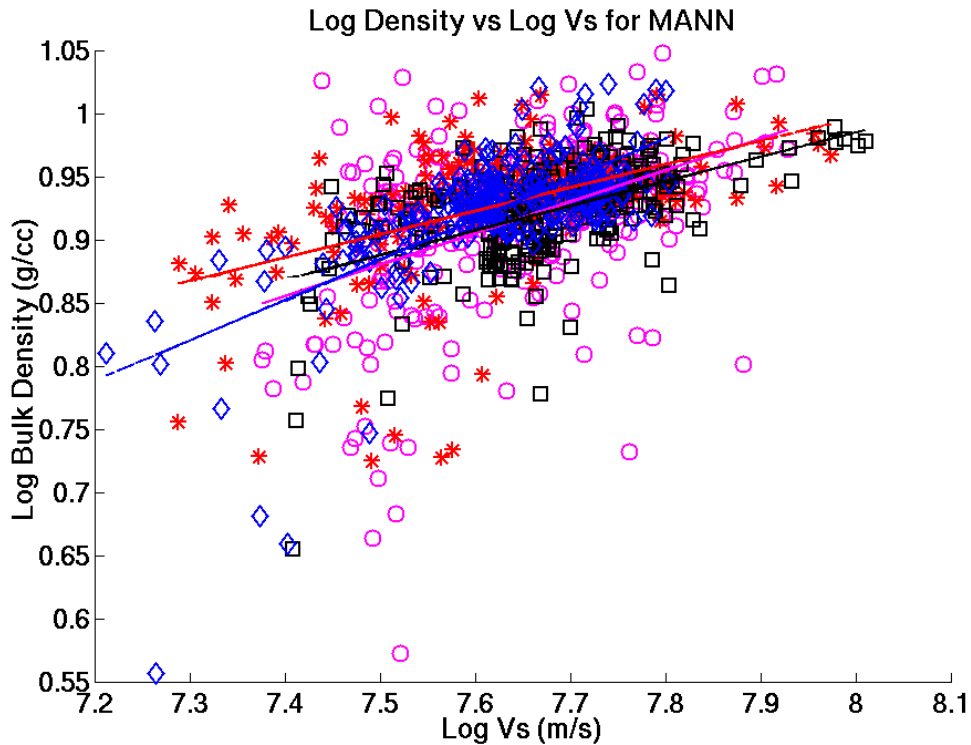


Figure 3. Log density versus Vs for the 08-08 (O), 09-08 (\*), 04-16 (□), and 12-16 (◇) wells for the Mannville.

Figure 4 shows the logarithm density versus the logarithm of S-wave velocity for the 08-08, 09-08, 04-16, and 12-16 wells for the Top of the Glauconitic (GLCTOP) and shows the best-fit lines for each wells. The equations derived for this data are as follows:

$$08-08 \quad \rho=0.47Vp^{0.05} \quad (14)$$

$$09-08 \quad \rho=0.88Vp^{0.002} \quad (15)$$

$$04-16 \quad \rho=-0.002Vp^{2.60} \quad (16)$$

$$12-16 \quad \rho=0.16Vp^{0.69} \quad (17)$$

$$\text{all wells} \quad \rho=0.38Vp^{0.11} \quad (18)$$

The data for the 12-16 and the 09-08 wells have a definite trend with relatively small scatter around the best-fit line, although the equations for these data do not comply with that of Gardner's equation. The data for the 08-08 and 04-16 wells are greatly scattered about their corresponding best-fit lines and also do not relate closely to Gardner's equations. There is a huge uncertainty in the coefficients. Equation (18) for 'all wells' corresponds to Gardner's equation best. The density values are lower for the 08-08 and 09-08 wells than those values for the 04-16 and 12-16 wells. This could indicate that the 08-08 and 09-08 wells have greater porosity than the 04-16 and 12-16 wells.

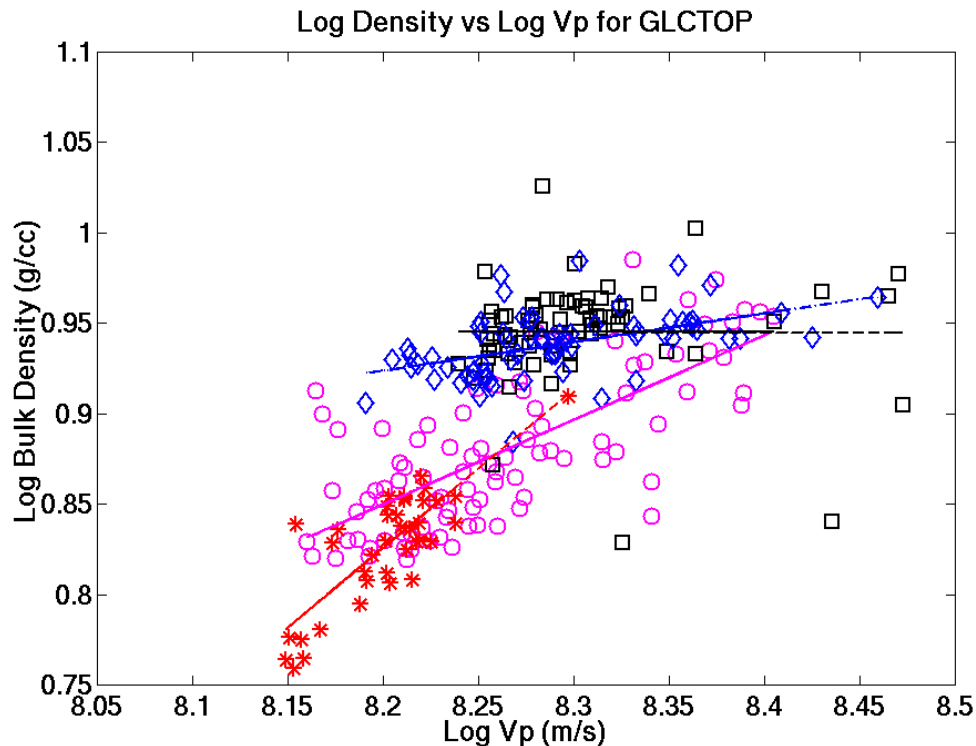


Figure 4. Log density versus Vp for the 08-08 (O), 09-08 (\*), 04-16 (□), and 12-16 (◇) wells for the Top of the Glauconitic.

Figure 5 shows density versus neutron porosity ( $\phi$ ) sandstone for the 08-08, 09-08, 04-16, and 12-16 for the Top of the Glauconitic (GLCTOP) and the corresponding best-fit lines through the data. The equations for the best-fit lines and the corresponding correlation coefficients ( $r$ ) are as follows:

08-08	$\rho=2210+992\phi$	$r=0.364$ (19)
09-08	$\rho=2057+1149\phi$	$r=0.688$ (20)
04-16	$\rho=2472+397\phi$	$r=0.185$ (21)
12-16	$\rho=2740-733\phi$	$r=-0.574$ (22)

The 09-08 data shows less scatter about the best-fit line than the data for the other wells. The 08-08 and 04-16 data have low correlation between density and porosity. This could be explained by the use of the neutron porosity log, which is affected by clays and fluid content. The 08-08 well is a gas/oil producer and the 04-16 well is shale plugged. The 08-08 data shows the cluster of data for gas and for the quartzose channel. The 08-08 gas has low density and low neutron porosity. Generally, there should be an inverse correlation between density and porosity. Again, the data for the 12-16 well corresponds best to these parameters with a relatively high negative correlation.

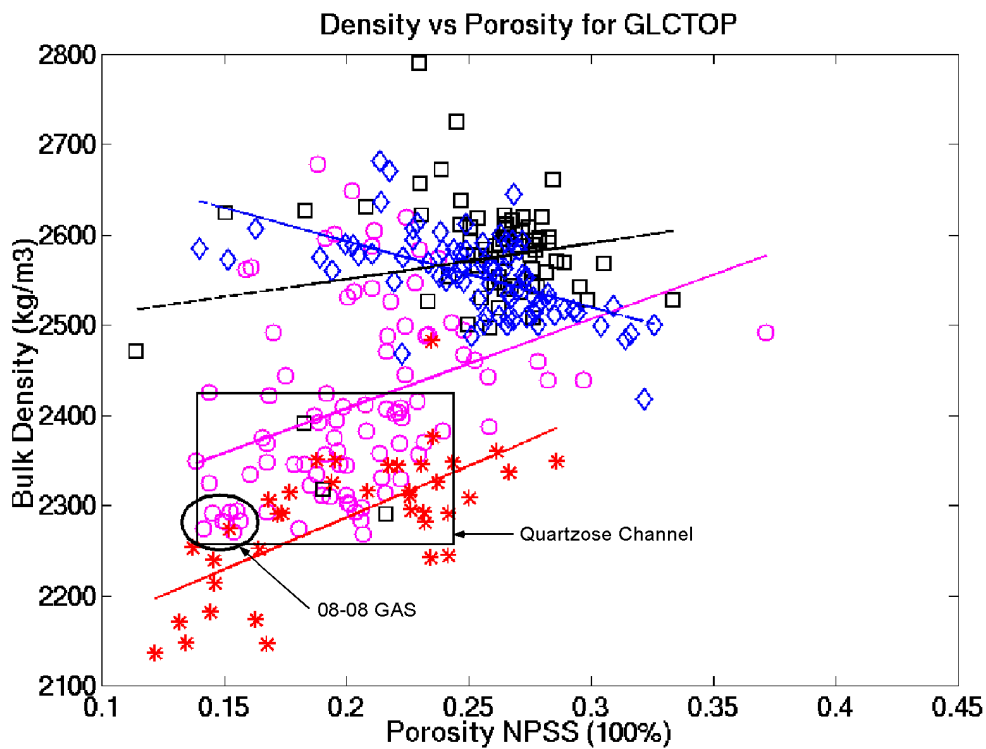


Figure 5. Density versus porosity for the 08-08 (O), 09-08 (\*), 04-16 (□), and 12-16 (◇) wells for the Top of the Glauconitic.

Figure 6 shows density versus calculated Poisson's ratio for the 08-08, 04-16, and 12-16 wells for the Top of the Glauconitic (GLCTOP) and the corresponding best-fit lines. The equations for the best-fit lines and the corresponding correlation coefficients (r) are as follows:

08-08	$\rho=2200+989\sigma$	$r=0.433$ (23)
04-16	$\rho=2150+1447\sigma$	$r=0.470$ (24)
12-16	$\rho=2746-664\sigma$	$r=-0.398$ (25)

All data of the three wells have wide spread scatter about the corresponding best-fit lines. When comparing the data of Figure 5 with that of Figure 6, the trends of the best-fit lines are very similar for each plot. Poisson's ratio values tend to be higher in 'soft' material. Therefore we would expect the values for the oil/gas 08-08 well to have higher values than is shown, but these values can be affected by pore fluids, porosity and lithology. Poisson's ratio shown here is calculated from the Vp and Vs logs and could be slightly higher for the 08-08 and 04-16 data.

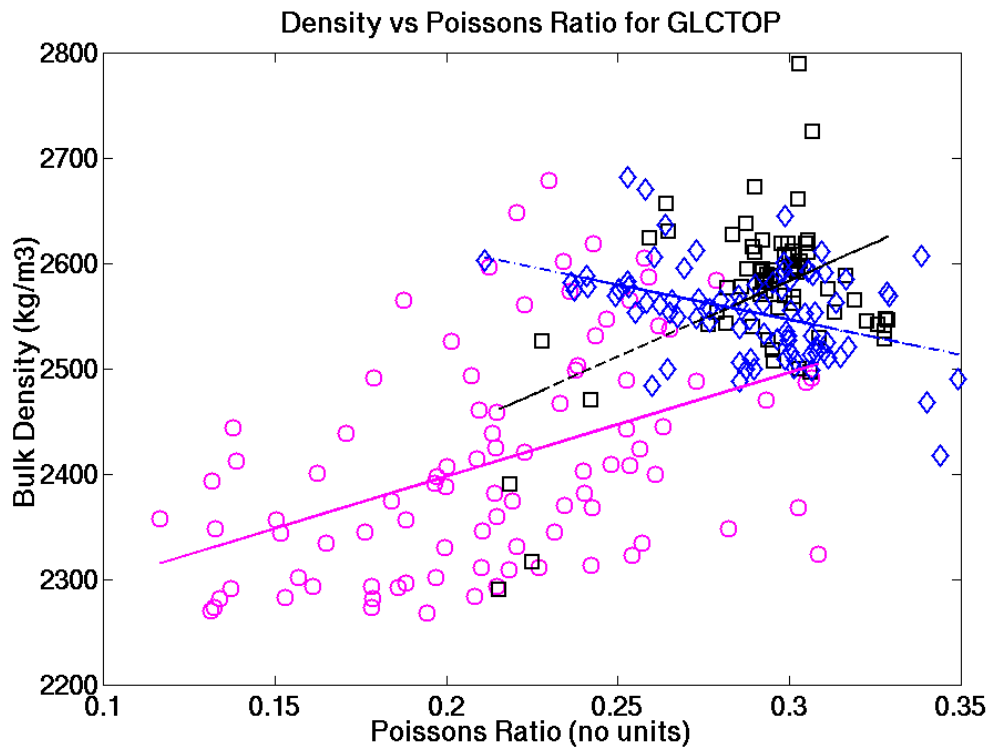


Figure 6. Density versus Poisson's ratio for the 08-08 (O), 04-16 ( $\square$ ), and 12-16 ( $\diamond$ ) wells for the Top of the Glauconitic.

Figure 7 shows the P-wave sonic and the density logs for the 04-16 well in depth. The slowness units for the P-wave sonic are shown at the bottom. The important point is that the peaks of the density log and the P-wave log should be opposite to each other at the same depth. When examining these logs, it appears that the density log has been slightly bulk shifted down in comparison to the P-wave log. This is also evident in the corresponding 08-08 logs. This would affect the log density versus log Vp figures.

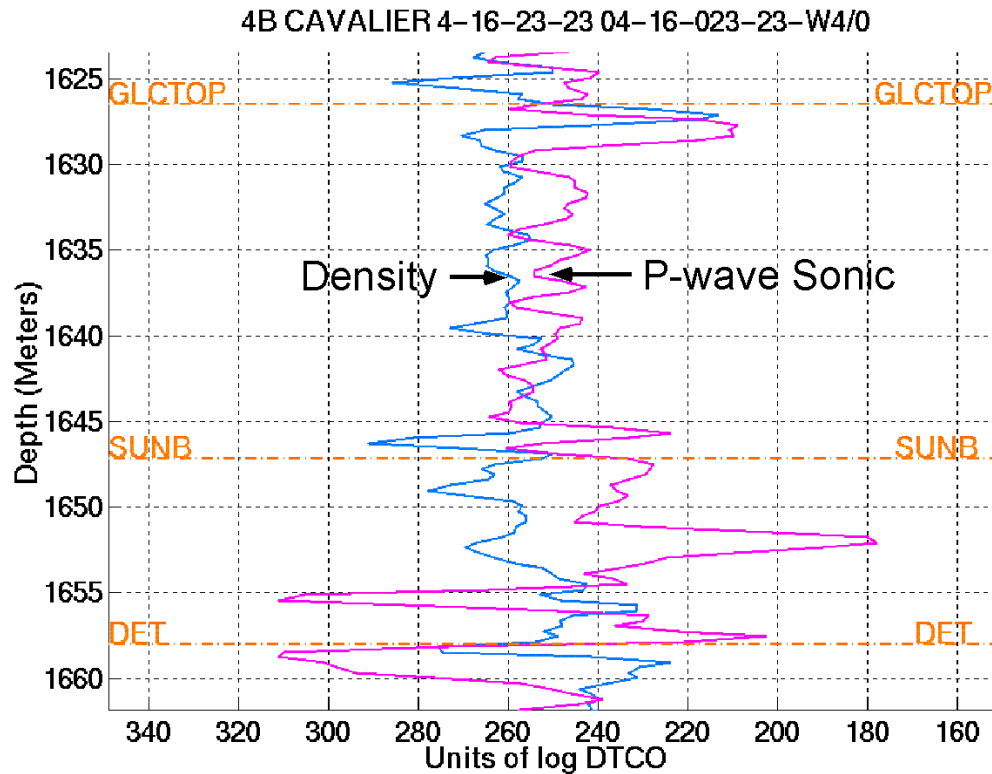


Figure 7. Density and P-wave sonic logs. The density log is the one on the right within the GLCTOP formation and the P-wave sonic is on the left. Note the slight downward bulk shift of the density log relative to the P-wave sonic log.

The measured log density - log Vp equations conform fairly well to Gardner's equations in the Mannville member, but tend to vary greatly within the Glauconitic member (upper channel). Similar plots for the lithic channel (LITHCH) (middle channel) and the Glauconitic porous sandstone (GLCSS) (lower channel) show great deviations from Gardner's empirical relationship. These channels should be separated into even finer increments of lithology in order to differentiate particular trends and perform regression analysis.

The correlation coefficients for Vp versus Vs within the Glauconitic channel show high correlation for the 12-16 ( $r=0.906$ ) and 04-16 ( $r=0.916$ ) wells, but considerably lower for the 08-08 ( $r=0.645$ ) well. This is understandable considering S-waves do not propagate through fluids, which would be present in the 08-08 well.

Potter and Stewart (1998) found that when comparing measured density coefficients with those of Gardner's equation for the same logs, with intervals from the top of the Mannville to the Mississippian, that they matched very well.

## CONCLUSIONS

The plots that correspond to Gardner's equations vary widely. The coefficients of the measured equations for 'all wells' corresponding to those of Gardner's were within reason for the Mannville member, but varied orders of magnitude apart within the

three different valley systems of the Glauconitic member. Gardner's empirical relationship is generally used for predicting density when not available and tends to deviate when affected by lithology, porosity, and pore fluids.

### **FUTURE WORK**

When this project was in the initial stages, it was expected that the borehole log data from PanCanadian would be ample. Since this data did not have an appropriate log suite, logs from QCData were acquired. After editing the public domain well logs, it was evident the certain corrections were required to obtain valid conclusions, which entail significantly more work to achieve. Notably, the Shear-wave logs must be processed correctly from the dipole sonics taking into consideration the variation of the full-wave form sonic and dipole sonic logs. Different tools give different responses and in the older tools cycle skipping is of major concern. Also, analyses of various cross-plots needs to completed. Core samples must be taken into consideration when investigating smaller formation intervals. Regression analysis of this data would allow better understanding of which parameters or elastic constants to be considered.

### **ACKNOWLEDGEMENTS**

We would like to thank the CREWES sponsors for their support and PanCanadian Petroleum Limited for the relevant data. We would also like to thank Rudi Meyer for related discussions.

### **REFERENCES**

- Gardner, G.H.F., Gardner, L.W., and Gregory, A.R., 1974, Formation velocity and density – The diagnostic basics for stratigraphic traps: *Geophysics*, 39, 770-780.
- Miller, S.L.M. and Stewart, R.R., 1990, Effects of lithology, porosity and shaliness on P- and S-wave velocities from sonic logs: *Can. J. Expl. Geophys.*, 26, 94-103.
- Pickett, G.R., 1963, Acoustic character logs and their applications in formation evaluation: *J. Petr.Tech.*, June, 659-667.
- Potter, C.C. and Stewart, R.R., 1998, Density predictions using Vp and Vs sonic logs: CREWES Research Report 1998, Ch. 10.
- Rafavich, F., Kendall, C.H.St.C., and Todd, T.P., 1984, The relationship between acoustic properties and the petrographic character of carbonate rocks: *Geophysics*, 49, 1622-1636.
- Sheriff, R.E., 1991, *Encyclopedic Dictionary of Exploration Geophysics*, Third Ed., SEG.
- Sheriff, R.E., and Geldart, L.P., 1995, *Exploration Seismology*, Second Edition: Cambridge University Press, New York, NY.